Dynamic Compression Augments Interstitial Transport of a Glucose-Like Solute in Articular Cartilage

Robin C. Evans and Thomas M. Quinn
Cartilage Biomechanics Group, Ecole Polytechnique Fédérale de Lausanne (EPFL), Lausanne, Switzerland

ABSTRACT Solute transport through the extracellular matrix is essential for cellular activities in articular cartilage. Increased solute transport via fluid convection may be a mechanism by which dynamic compression stimulates chondrocyte metabolism. However, loading conditions that optimally augment transport likely vary for different solutes. To investigate effects of dynamic loading on transport of a bioactive solute, triangular mechanical loading waveforms were applied to cartilage explants disks while interstitial transport of a fluorescent glucose analog was monitored. Peak-to-peak compression amplitudes varied from 5–50% and frequencies varied from 0.0006–0.1 Hz to alter the spatial distribution and magnitude of oscillatory fluid flow. Solute transport was quantified by monitoring accumulation of fluorescence in a saline bath circulated around the explant. Individual explants were subjected to a series of compression protocols, so that effects of loading on solute desorption could be observed directly. Maximum increases in solute transport were obtained with 10–20% compression amplitudes at 0.1 Hz; similar loading protocols were previously found to stimulate chondrocyte metabolism in vitro. Results therefore support hypotheses relating to increased solute transport as a mediator of the cartilage biological response to dynamic compression, and may have application in mechanical conditioning of cartilage constructs for tissue engineering.

INTRODUCTION

The mechanically functional extracellular matrix of adult articular cartilage is ~70–80% fluid, but avascular. Various solutes move through this matrix in support of chondrocyte biological activities, including nutrients, wastes, enzymes, inhibitors, cytokines, and matrix macromolecules. Interstitial transport of bioactive solutes over millimeter-length scales is of central biological importance in cartilage. Alterations in solute transport may therefore mediate chondrocyte metabolic responses to cartilage compression, affecting tissue homeostasis, degradation, and cell-mediated matrix remodeling.

Chondrocyte-mediated matrix assembly changes differentially in response to cartilage dynamic compression of varying amplitudes and frequencies. Joint immobilization and decreased loading in vivo can reduce proteoglycan synthesis and assembly (1–3), whereas exercise can increase cartilage proteoglycan content (2,3). Similarly, low amplitude (1–10%) compression of cartilage explants at 0.01–0.1 Hz stimulates matrix synthesis (4–8), whereas low amplitude compression at lower frequencies has no effect (4,5) or an inhibitory effect (8). The frequency dependence of the chondrocyte mechanotransduction response has been linked to oscillatory fluid flow distributions. Regions of highest upregulation of matrix synthesis are exposed to relatively high flow velocities (9,10). These effects are particularly dramatic at relatively high frequencies where stimulation of cell metabolism and fluid flows are localized to the radial edge of axially compressed explant disks (5,7,9). In addition to other possible mediators such as shear stresses, fluid pressurization, and cell-matrix interactions, augmented solute transport due to convection may therefore be a mechanism by which dynamic loading stimulates chondrocyte metabolism (4,10,11).

Cartilage dynamic compression combines matrix compaction together with interstitial fluid flow, and introduces time-varying solute-matrix interactions. Compression-induced fluid flow is associated with augmented solute transport (12,13), whereas diffusion decreases with increasing compressive strain (14–16). Positive convection coefficients measured for 0.5–10 kDa dextrans in articular cartilage (17) indicate that dynamic compression can augment transport of some solutes. However, optimal loading conditions remain unclear for specific solutes of interest.

Our goals were to investigate effects of radially unconfined dynamic compression of cartilage explant disks on interstitial transport of a 342 Da fluorescent glucose analog. Compression was applied over a range of amplitudes and frequencies to vary the spatial distribution and magnitude of matrix strains and fluid flows. Accumulation of fluorescence in a saline bath around the explant was compared with theoretical solutions for estimation of solute partition and diffusion coefficients. Effects of dynamic compression on solute transport were observed directly for individual explants in a series of desorption experiments and interpreted in relation to previous studies of chondrocyte mechanotransduction.

MATERIALS AND METHODS

Osteochondral cores (5 mm diameter) were drilled from fresh humeral heads of 18-month-old cows. With a microtome (RM 2135, Leica, Wetzlar, Germany), the superficial layer was removed, then a 600 μm thick cartilage

Submitted January 3, 2006, and accepted for publication April 26, 2006.

Address reprint requests to Thomas M. Quinn, PhD, Cartilage Biomechanics Group AI 1234, EPFL Station 15, Lausanne, Switzerland. Tel.: 41-21-693-83-50; Fax: 41-21-693-86-60; E-mail: thomas.quinn@epfl.ch.

0006-3495/06/08/1541/07 $2.00

doi: 10.1529/biophysj.105.080366

sheet sliced, consisting of middle and deep zone matrix, to promote homogenous solute transport (18). Explants were stored at −20°C in phosphate buffered saline (PBS) with protease inhibitors (Complete, Boehringer Mannheim, Ingelheim, Germany) and 0.1 mg/mL sodium azide (Sigma, Buchs, Switzerland) until experimental use. Chondrocytes were therefore nonviable during experiments. Ten animals contributed explants to this study. Explants were placed overnight in 200 μL absorption baths containing the 342 Da fluorescent glucose analog 2-[*N*-(7-nitrobenz-2-oxa-1,3-diazol-4-yl)amino]-2-deoxy-D-glucose (2-NBDG; Molecular Probes, Eugene, OR), previously used to monitor cellular glucose uptake (19). Concentrations of 2-NBDG in absorption baths were 2.4–7.3 mM, similar to previous studies (20). After overnight equilibration, explants were punched to 4 mm diameter to minimize effects due to solute adsorption at explant radial edges.

For each explant, a 30-min compression and solute desorption protocol was followed on each of three days (Fig. 1). On days 1 and 3, desorption occurred during 0% static compression (relative to dissection thickness), whereas on day 2, dynamic compression was applied (below). Effects of dynamic relative to static compression were thereby directly observed for individual explants, whereas static compression protocols bracketing the dynamic compression provided a control for changing explant properties. Explants were reequilibrated overnight in solute baths between compression protocols.

For compression and desorption, explant disks were subjected to radially unconfined axial compression (Fig. 2). A nonporous platen was placed on the explant upper surface to ensure radially directed fluid and solute transport. Compression was applied with a displacement actuator (PM-500 C, Newport, Irvine, CA) in series with a load cell (Sensotec, Columbus, OH) interfaced with virtual instrumentation software (LabView, National Instruments, Austin, TX). Dynamic compression was applied with a triangular waveform (between 0% and a predetermined maximum) over a range of amplitudes and frequencies (Fig. 3). Peak-to-peak amplitudes included 5%, 10%, 20% (moderate physiological loading (21,22)), and 50% (extreme in vivo loading (23)). Compression frequencies included 0.1 Hz (previously found to stimulate chondrocyte metabolism (4)), 0.01 Hz, and 0.0006 Hz (near the intrinsic rate of cartilage matrix stress relaxation (24)).

A small offset compression to 0% from free-swelling conditions was applied at 10 μm/s with the explant in a dry compression chamber. About 30 s later, when oscillatory dynamic compression began (time $t = 0$), 10 mL of PBS was introduced and continuously recirculated through the compression chamber using a peristaltic pump to promote a zero-concentration boundary for radially directed solute transport (desorption bath concentration was at most 0.001× that of the absorption bath). At 5-min intervals, 100 mL of desorption bath was removed in triplicate for fluorescence measurement with a plate reader (PerkinElmer, Wellesley, MA) calibrated to solute concentration with standards of 2-NBDG in PBS.

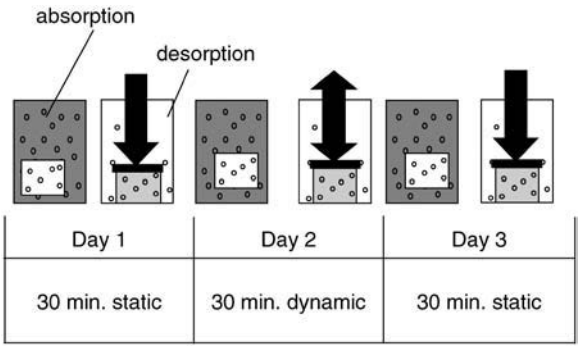

FIGURE 1 Schematic of three-day experimentation sequence. A 30-min compression protocol was applied to cartilage explant disks each day. On days 1 and 3, 0% static compression was applied, whereas on day 2, dynamic compression was applied. Explants were equilibrated overnight in solute absorption baths before each compression and desorption protocol.

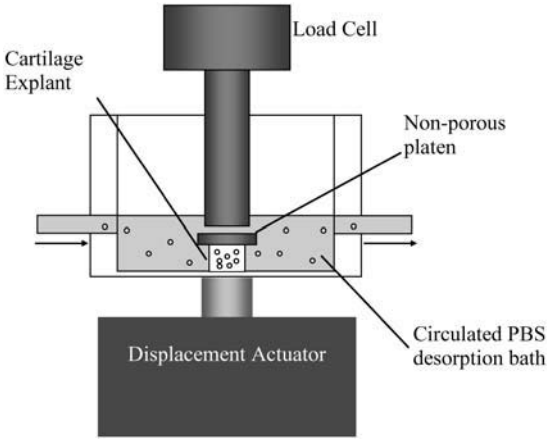

FIGURE 2 Schematic of experimental apparatus. Cartilage explant disks containing a fluorescent glucose analog were mounted in radially unconfined axial compression in a well-mixed PBS bath. Compression was applied with a precision displacement actuator in series with a load cell. A nonporous platen was placed over the explant to ensure radially directed fluid flow and solute transport from the explant into the PBS bath.

The effective diffusivity (D) of 2-NBDG in cartilage was estimated using day 1 desorption kinetics. With interstitial solute concentration c defined as the number of molecules per unit volume of tissue fluid, D related area-averaged solute flux Γ to ∇c:

$$\Gamma = -D\frac{\partial c}{\partial r}, \tag{1}$$

where c varied only with radial position r in explant disks and t. Solute conservation required

$$\frac{\partial c}{\partial t} = \frac{D}{\phi}\left[\frac{1}{r}\frac{\partial}{\partial r}\left(r\frac{\partial c}{\partial r}\right)\right], \tag{2}$$

where ϕ was explant fluid volume fraction. With conditions of initially uniform concentration ($c(r, t = 0) = c_0$) and a zero concentration boundary ($c(r = R, t) = 0$) the solution to Eq. 2 may be written (25)

$$c(r,t) = \sum_{m=1}^{\infty} \frac{2c_0}{q_m J_1(q_m)} \cdot J_0\left(q_m \frac{r}{R}\right) e^{-t/\tau_m}, \tag{3}$$

where the q_m represent zeros of the Bessel function J_0 and

$$\tau_m = \frac{\phi R^2}{D q_m^2}. \tag{4}$$

Integrating to determine desorbed solute concentration (c_b) in a bath with volume V_b provides

$$c_b(t) = c_{b0} + \frac{c_0 \pi R^2 H \phi}{V_b}\left[1 - \sum_{m=1}^{\infty} \frac{4}{q_m^2} e^{-t/\tau_m}\right], \tag{5}$$

where H was explant disk thickness. Disk radius R was estimated from the punched diameter and previous measurements of cartilage Poisson's ratio (26). Fluid volume fraction ϕ was determined from free-swelling fluid volume fraction and explant volumetric strain under static compression. The diffusion coefficient D was thereby determined as the only free parameter in a least-squares fit of Eq. 5 with experimental data. Reduced volume of the desorption bath due to sampling for fluorescence measurements was accounted for as in previous work (27).

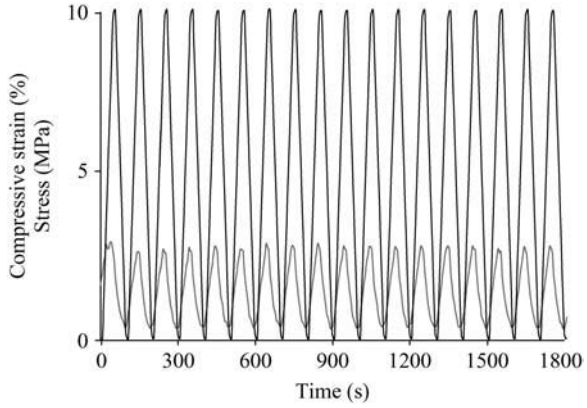

FIGURE 3 Dynamic compression was applied in a symmetrical triangular waveform with compressive strain (*solid line*) defined relative to explant dissection thickness. The peak-to-peak amplitude of compression was one of 5, 10, 20, or 50%, whereas the frequency was one of 0.0006, 0.01, or 0.1 Hz. Explant compressive stress (*shaded line*) was continuously monitored with the load cell.

A final absorption and desorption to equilibrium were performed to determine equilibrium partitioning of 2-NBDG. With the partition coefficient K defined at equilibrium by $c = Kc_a$, where c_a was absorption bath solute concentration, then by analogy with previous work (16)

$$K = \frac{V_d c_d}{V_0 \phi (c_a - c_d)}, \quad (6)$$

where V_d and c_d were volume (1 mL) and equilibrium solute concentration in the desorption bath, and V_0 was explant free-swelling volume (estimated from control studies as 1.2 times the dissection volume).

After the partitioning measurement, explants were left overnight in PBS with protease inhibitors, blotted on tissue to remove surface fluid, weighed, lyophilized, and weighed again. Free-swelling fluid volume fractions were determined from the difference between wet and dry weights assuming 1 g/mL density of tissue fluid. Explants were then digested overnight at 60°C in 1 mL PBS containing 125 μg/mL papain (Sigma). Explant glycosaminoglycan (GAG) content was assayed by established methods (28) to determine GAG weight fraction (mg GAG/explant wet weight).

For analysis of desorption kinetics, bath solute concentrations at each time point during dynamic compression on day 2 and static compression on day 3 were normalized to corresponding values for static compression on day 1. Normalized bath solute concentrations were compared with unity using a single-group t-test to identify effects of loading. Differential effects of compression amplitude and frequency on solute desorption rates were assessed by two-way ANOVA of normalized desorption bath solute concentrations at the 30 min time point. Validity of t-tests and ANOVA was supported by normal distribution analysis. To explore influences of cartilage matrix density and mechanical properties on solute desorption rates and diffusivities (26), relationships among these variables were evaluated using the Pearson correlation coefficient (ρ) for paired data sets. Matrix density was characterized by GAG weight and fluid volume fractions, whereas mechanical properties were characterized by peak-to-peak stresses during steady-state dynamic compression. Differences and correlations were considered significant at $t < 0.05$ and $p < 0.05$.

RESULTS

Desorption kinetics of 2-NBDG from cartilage explants under 0% static compression were indistinguishable on days 1 and 3. For all time points, no differences were detected by ANOVA between bath solute concentrations on days 1 and 3, regardless of loading applied on day 2 (Fig. 4). Therefore changes in solute desorption measured on day 2 (below) were due to dynamic loading and not changing explant properties.

During dynamic compression, liftoff was sometimes observed between the loading post and platen at higher frequencies (Fig. 2), but there was no visible liftoff between the platen and cartilage. In fact, when explants were subsequently removed from the apparatus, they were often difficult to separate from the platen due to suction effects (29). Therefore, boundary conditions for radially directed transport appeared well-preserved during dynamic compression.

For dynamic loading at 0.1 Hz, normalized desorption bath solute concentrations were significantly greater than 1 for 10% amplitude at all times, and for 5 and 20% amplitudes for some time points (Fig. 5 *A*). Increased desorption rate of 2-NBDG from cartilage explants was also evident for 0.01 Hz loading, where normalized bath concentrations were significantly greater than 1 for 5% and 20% amplitudes at several time points (Fig. 5 *B*). For 0.0006 Hz dynamic loading, no sustained significant increase in normalized bath concentration was observed (Fig. 5 *C*).

Two-way ANOVA of normalized bath solute concentration after 30 min of dynamic loading indicated that compression frequency was the dominant factor influencing enhanced 2-NBDG transport ($p < 0.05$), with significant interaction between frequency and amplitude ($p < 0.001$). For all amplitudes, desorption rates tended to increase as compression frequency increased from 0.0006 to 0.1 Hz (Fig. 6). After 30 min, the most significant increases in desorption occurred for 10 and 20% compression amplitudes at 0.1 Hz (33 ± 11% and 37 ± 8%) and for 5% amplitude at 0.01 Hz (12 ± 4%). Although not statistically significant, dynamic compression at 50% amplitude and 0.0006 Hz appeared to decrease solute desorption rates compared to 0%

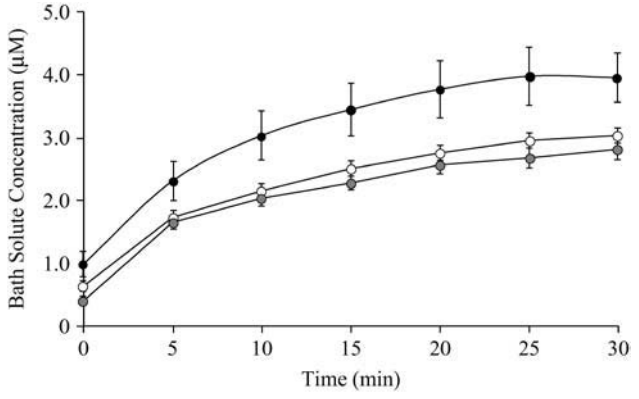

FIGURE 4 Solute desorption kinetics from cartilage explants subjected to 0% static compression on days 1 (*open circles*) and 3 (*shaded circles*), and dynamic compression with 10% amplitude at 0.1 Hz on day 2 (*solid circles*). Mean ± SE, $n = 10$.

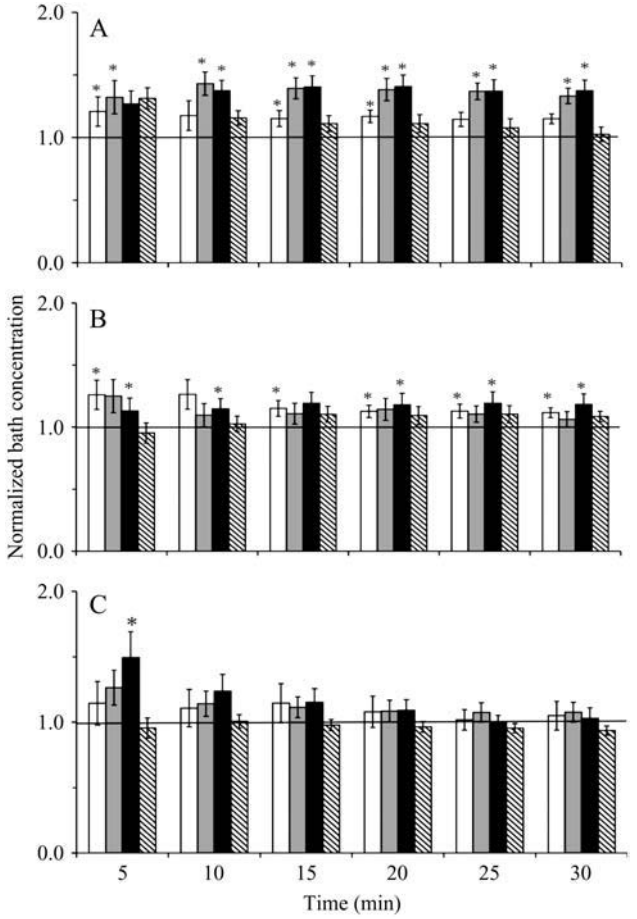

FIGURE 5 Bath solute concentrations on day 2 (during dynamic compression) normalized to those on day 1 (during static compression) for each explant. Each group of four bars represents, from left to right, 5, 10, 20, and 50% dynamic compression amplitude. Dynamic compression frequencies were (*A*) 0.1 Hz, (*B*) 0.01 Hz, and (*C*) 0.0006 Hz. Asterisks above bars indicate significant differences between the associated data and 1 ($p < 0.05$, mean ± SE, $n = 10$).

static compression (Fig. 6). No consistent significant correlations were detected between desorption rates of 2-NDGB for each compression protocol and cartilage matrix density (characterized by GAG weight and fluid volume fractions).

Partition coefficients for 2-NBDG in free-swelling cartilage were normally distributed around 1.51 ± 0.01 ($n = 66$). K was significantly greater than 1, suggesting attractive interactions between 2-NBDG and cartilage matrix. However, K was not significantly correlated with matrix density.

Diffusivities for 2-NBDG in cartilage under 0% static compression were the only data acquired that were not normally distributed. The median 50% range of D was 524–1389 $\mu m^2/s$ ($n = 124$). Within each dynamic compression group, D correlated inversely with normalized desorption bath solute concentrations at 30 min ($|\rho| = 0.24$–0.54, $n = 12$) and with steady-state peak-to-peak stresses at 0.1 and 0.01 Hz ($|\rho| = 0.25$–0.35, $n = 8$). D was not significantly correlated with matrix density.

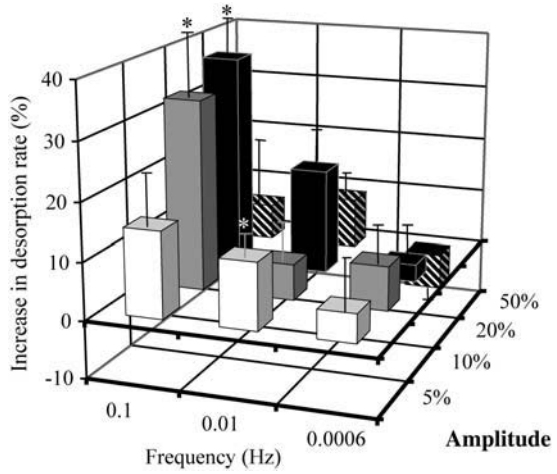

FIGURE 6 Fractional increases in rates of solute desorption from cartilage explant disks after 30 min of dynamic compression, relative to desorption under static compression. Open bars indicate 5% compression amplitude, shaded bars, 10%; solid bars, 20%; and striped bars, 50%. Significant changes in rates of solute transport into the desorption bath are indicated by asterisks ($p < 0.05$).

DISCUSSION

Previous studies suggest that dynamic compression may augment solute transport through cartilage matrix (6,12,17). Current results demonstrate that dynamic compression can increase interstitial transport rates of a 342 Da glucose analog in cartilage explants. Furthermore, loading amplitudes and frequencies that most dramatically increased solute transport corresponded to those known to stimulate chondrocyte-mediated matrix synthesis (4). These findings support hypotheses regarding increases in bioactive solute transport as a mediator of cartilage biological responses to mechanical compression.

For simulating nutrient transport into cartilage, current methods may appear unsatisfactory since transport was directed outward. However, similar effects are expected whether solute enters or leaves the tissue. Standard equations governing radially directed solute transport (by diffusion and convection) in dynamically compressed cartilage disks are linear in the concentration (17)

$$\phi\frac{\partial c}{\partial t} = \frac{D}{r}\left[\frac{\partial}{\partial r}\left(r\frac{\partial c}{\partial r}\right)\right] + \left(\frac{\partial U}{\partial r} + \frac{U}{r}\right)(1-\omega)c - U\omega\frac{\partial c}{\partial r}, \tag{7}$$

where $U(r,t)$ is area-averaged interstitial fluid velocity and ω is the convection coefficient (defined so that area-averaged solute convective flux is ωcU (17)). Therefore, any two valid solutions for $c(r,t)$ can be superposed to obtain another valid solution. With this in mind, consider experiments identical to the study presented here except where the desorption bath has the same solute concentration as the overnight equilibration bath. No important changes in interstitial solute concentrations will occur. But the difference between this situation and the

experiments actually performed corresponds to the case where interstitial solute concentration is initially zero and increases due to inward-directed transport from a high concentration bath during loading. Therefore, wherever solute exited cartilage during current experiments, it would be expected to enter during an ''oppositely oriented'' protocol. One may therefore conclude that current findings apply equally well for compression-induced increases of 2-NBDG transport into cartilage.

Effects of dynamic compression on 2-NBDG transport in cartilage were highly dependent on loading amplitudes and frequencies. The most significant increases in solute desorption rates occurred for amplitudes of 10–20% at 0.1 Hz, and for 5% amplitude at 0.01 Hz (Fig. 6). These loading frequencies exceed the intrinsic ''gel diffusion'' frequency (f_{gd}) of mechanical relaxation in cartilage (24), given by

$$f_{gd} = \frac{H_A k}{d^2}, \tag{8}$$

where H_A and k represent matrix elastic modulus and hydraulic permeability, and d is a characteristic distance. For typical values of H_A and k (10,24), f_{gd} is ~0.001 Hz for a cartilage explant of millimeter dimensions. Interstitial fluid flows induced by dynamic compression at frequencies greater than f_{gd} involved relatively high velocities localized to the radial edge of cartilage explant disks (5,30). In contrast, matrix deformations under 0.0006 Hz loading were quasistatic, involving relatively low velocity flows distributed more broadly across the disk radius (5). Increasing compression frequency was the main factor contributing to increased solute transport (Figs. 5 and 6), suggesting that high frequency oscillatory flows near that explant disk radial edge affected solute transport more than quasistatic flows.

These insights may be formalized somewhat by consideration of the Peclet number (Pe) for solute transport in dynamically compressed cartilage. This dimensionless parameter represents the relative significance of solute convection versus diffusion

$$Pe = \frac{\omega U d}{D}. \tag{9}$$

For $Pe < 1$, diffusion dominates transport, whereas for $Pe > 1$, convection is more important. During the compression phase of an axially loaded, radially unconfined cartilage disk, fluid velocity at the radial edge (explant volume change rate divided by radial surface) scales approximately with the product ARf, where A and f are dynamic compression strain amplitude and frequency, and d may be represented by disk radius R. Using Eq. 8, the Peclet number may therefore be estimated by

$$Pe = \frac{Af}{f_{gd}}\left(\omega\frac{H_A k}{D}\right). \tag{10}$$

For typical values of material properties (10,24), convection coefficients (17), and 2-NBDG diffusivities, the term in brackets in Eq. 10 is near unity. Therefore, dynamic compression is expected to introduce significant convective augmentation of interstitial 2-NBDG transport roughly when Af exceeds f_{gd}, consistent with our results (Fig. 6). These scaling arguments neglect important aspects of explant mechanics (e.g., Poisson's ratio, compression-dependent nonlinear properties (22)) and solute transport (e.g., dispersion in oscillating flows (31)), but nevertheless suggest a reasonable starting point in searches for loading conditions that optimize solute transport in cartilage.

Very high compression amplitudes appeared to be associated with decreased solute transport: compression at 50% amplitude did not significantly increase 2-NBDG desorption rates for any loading frequencies (Fig. 6). Although large deformations involve displacements of large amounts of fluid, they can also hinder solute transport due to steric interactions (15,16). Decreased hydraulic permeability due to matrix compaction may also decrease fluid velocities and diminish effects of convection. Furthermore, large compressive strains applied at high strain rates can induce cartilage matrix damage (32). For the most extreme dynamic compression condition involving 50% amplitude at 0.1 Hz, significant increases in explant fluid volume fraction (to $\phi = 0.84 \pm 0.01$) were detected. Even in this case, no significant changes in solute desorption kinetics were evident between days 1 and 3, but these changes suggest matrix damage. Therefore, contributions of dynamic compression to augment solute transport and stimulate chondrocyte metabolism may ultimately be limited by onset of mechanical injury.

Results highlight relationships between increases in solute transport and chondrocyte-mediated matrix synthesis in response to cartilage dynamic compression. In the study presented here, the highest solute desorption rates were associated with 0.01–0.1 Hz frequencies and relatively low amplitude (5–20%) compression (Figs. 5 and 6). These ''optimal'' mechanical conditions for 2-NBDG transport correspond to loading conditions seen to increase cell-mediated matrix synthesis in previous work (4–8). Together with the colocalization of increased cell metabolism and fluid flow (5,7,9), current results strongly support a role for convective augmentation of solute transport as a mediator of chondrocyte mechanotransduction. Future work may be motivated by observations that maximum solute desorption rates were found at the experimental extreme of 0.1 Hz. Higher frequencies may promote still greater increases in solute transport and stimulation of cell metabolism. Frequencies near 1 Hz would be of particular interest because of their relationship to physiological gait cycles.

Measured transport coefficients of 2-NBDG were generally consistent with previous findings. The equilibrium partition coefficient of glucose in cartilage was previously measured at 0.5–0.9 (27,33), somewhat less than current findings of 1.51 ± 0.01 for 2-NBDG. Chemical differences between glucose and 2-NBDG may explain the apparently attractive interaction between 2-NBDG and cartilage matrix (indicated by $K > 1$), which has previously been observed

for other fluorescent solutes (16) but was not evident for glucose (27,33). No correlation was observed between K of 2-NBDG and explant GAG weight fraction, suggesting that solute-matrix interactions may be nonspecific rather than electrostatic in origin. Current findings for diffusivity (D) of 2-NBDG in cartilage were mostly (median 50%) within the range of 524–1389 $\mu m^2/s$. Values of D for radiolabeled glucose in cartilage have been measured in the range 320–740 $\mu m^2/s$ (13,34). Structural differences between glucose and 2-NBGD may also contribute to differences in D.

Primary sources of measurement error arose from indirect determination of explant geometry. Differences from the mean Poisson's ratio determined in pilot studies may have perturbed estimates of compressed explant geometries, which then affected measured transport coefficients. Direct observation of explant geometry is preferable for accurate determination of K and D (17). However, this limitation does not compromise findings of increased transport rates of 2-NBDG in dynamically compressed cartilage, since effects were observed directly for individual explants.

Current findings indicate that interstitial transport of relatively small molecules may be augmented by cartilage dynamic compression. Previous studies have suggested that diffusion dominates interstitial transport of solutes with high diffusivities, whereas convection is most significant for transport of larger molecules with lower diffusivities (35). Current findings were consistent with this trend since within each dynamic compression group, solute diffusivity correlated inversely with normalized desorption bath solute concentration; in other words, dynamic compression-induced augmentation of 2-NBDG transport was greatest when diffusivities were smallest. In contrast with previous assumptions (12), current results therefore suggest that cartilage dynamic compression can significantly augment transport of solutes as small as glucose.

Our methods and others (11,17,18,35) provide means for further exploration of relationships between cartilage dynamic compression and solute transport. Interstitial glucose transport in articular cartilage and engineered cartilage-like tissues plays a central role in chondrocyte metabolism (20,34,36–40). Chondrocytes in vivo are exposed to diminishing concentrations of glucose with increasing depth from the articular surface, since it is consumed as it moves through the matrix from the synovial fluid (13). Solute consumption and production introduce complexities in transport phenomena beyond those considered in the study presented here. However, the glucose analog 2-NBDG could be useful for monitoring interstitial and transmembrane transport, and cell metabolism (19,38). Our methods and results may therefore aid in identifying optimal loading regimes for augmented transport of various solutes in cartilage, with implications for physiological understanding and improvements in cartilage tissue engineering.

This work was supported by a grant from the Swiss National Science Foundation.

REFERENCES

1. Palmoski, M., E. Perricone, and K. D. Brandt. 1979. Development and reversal of a proteoglycan aggregation defect in normal canine knee cartilage after immobilization. *Arthritis Rheum.* 22:508–517.
2. Tammi, M., A. M. Saamanen, A. Jauhiainen, O. Malminen, I. Kiviranta, and H. Helminen. 1983. Proteoglycan alterations in rabbit knee articular cartilage following physical exercise and immobilization. *Connect. Tissue Res.* 11:45–55.
3. Kiviranta, I., J. Jurvelin, M. Tammi, A. M. Saamanen, and H. J. Helminen. 1987. Weight bearing controls glycosaminoglycan concentration and articular cartilage thickness in the knee joints of young beagle dogs. *Arthritis Rheum.* 30:801–809.
4. Sah, R. L. Y., Y. J. Kim, J. Y. H. Doong, A. J. Grodzinsky, A. H. K. Plaas, and J. D. Sandy. 1989. Biosynthetic response of cartilage explants to dynamic compression. *J. Orthop. Res.* 7:619–636.
5. Kim, Y. J., R. L. Y. Sah, A. J. Grodzinsky, A. H. K. Plaas, and J. D. Sandy. 1994. Mechanical regulation of cartilage biosynthetic behavior: physical stimuli. *Arch. Biochem. Biophys.* 311:1–12.
6. Bonassar, L. J., A. J. Grodzinsky, E. H. Frank, S. G. Davila, N. R. Bhaktav, and S. B. Trippel. 2001. The effect of dynamic compression on the response of articular cartilage to insulin-like growth factor-I. *J. Orthop. Res.* 19:11–17.
7. Quinn, T. M., A. J. Grodzinsky, M. D. Buschmann, Y. J. Kim, and E. B. Hunziker. 1998. Mechanical compression alters proteoglycan deposition and matrix deformation around individual cells in cartilage explants. *J. Cell Sci.* 111:573–583.
8. Palmoski, M. J., and K. D. Brandt. 1984. Effects of static and cyclic compressive loading on articular cartilage plugs in vitro. *Arthritis Rheum.* 27:675–681.
9. Buschmann, M. D., Y. J. Kim, M. Wong, E. Frank, E. B. Hunziker, and A. J. Grodzinsky. 1999. Stimulation of aggrecan synthesis in cartilage explants by cyclic loading is localized to regions of high interstitial fluid flow. *Arch. Biochem. Biophys.* 366:1–7.
10. Kim, Y. J., L. J. Bonassar, and A. J. Grodzinsky. 1995. The role of cartilage streaming potential, fluid flow, and pressure in the stimulation of chondrocyte biosynthesis during dynamic compression. *J. Biomech.* 28:1055–1066.
11. Quinn, T. M., A. E. Dunlop, and R. C. Evans. 2002. New approaches to solute transport measurement in mechanically loaded articular cartilage. *JSME International Journal Series C.* 45:944–951.
12. O'Hara, B. P., J. P. Urban, and A. Maroudas. 1990. Influence of cyclic loading on the nutrition of articular cartilage. *Ann. Rheum. Dis.* 49:536–539.
13. Maroudas, A., P. Bullough, S. A. Swanson, and M. A. Freeman. 1968. The permeability of articular cartilage. *J. Bone Joint Surg. Br.* 50:166–177.
14. Burstein, D., M. L. Gray, A. L. Hartmann, R. Gipe, and B. D. Foy. 1993. Diffusion of small solutes in cartilage as measured by nuclear magnetic resonance (NMR) spectroscopy and imaging. *J. Orthop. Res.* 11:465–478.
15. Quinn, T. M., P. Kocian, and J. J. Meister. 2000. Static compression is associated with decreased diffusivity of dextrans in cartilage explants. *Arch. Biochem. Biophys.* 384:327–334.
16. Quinn, T. M., V. Morel, and J. J. Meister. 2001. Static compression of articular cartilage can reduce solute diffusivity and partitioning: implications for the chondrocyte biological response. *J. Biomech.* 34:1463–1469.
17. Evans, R. C., and T. M. Quinn. 2006. Solute convection in dynamically compressed cartilage. *J. Biomech.* 39:1048–1055.
18. Leddy, H. A., and F. Guilak. 2003. Site-specific molecular diffusion in articular cartilage measured using fluorescence recovery after photobleaching. *Ann. Biomed. Eng.* 31:753–760.
19. Yoshioka, K., H. Takahashi, T. Homma, M. Saito, K. B. Oh, Y. Nemoto, and H. Matsuoka. 1996. A novel fluorescent derivative of glucose applicable to the assessment of glucose uptake activity of Escherichia coli. *Biochim. Biophys. Acta.* 1289:5–9.
20. Otte, P. 1991. Basic cell metabolism of articular cartilage. Manometric studies. *Z. Rheumatol.* 50:304–312.

21. Armstrong, C. G., A. S. Bahrani, and D. L. Gardner. 1979. In vitro measurement of articular cartilage deformations in the intact human hip joint under load. *J. Bone Joint Surg. Am.* 61:744–755.

22. Park, S., C. T. Hung, and G. A. Ateshian. 2004. Mechanical response of bovine articular cartilage under dynamic unconfined compression loading at physiological stress levels. *Osteoarthritis Cartilage.* 12:65–73.

23. Herberhold, C., S. Faber, T. Stammberger, M. Steinlechner, R. Putz, K. H. Englmeier, M. Reiser, and F. Eckstein. 1999. In situ measurement of articular cartilage deformation in intact femoropatellar joints under static loading. *J. Biomech.* 32:1287–1295.

24. Armstrong, C. G., W. M. Lai, and V. C. Mow. 1984. An analysis of the unconfined compression of articular cartilage. *J. Biomech. Eng.* 106:165–173.

25. Crank, J. 1975. The mathematics of diffusion. Oxford University Press, Oxford.

26. Evans, R. C., and T. M. Quinn. 2005. Solute diffusivity correlates with mechanical properties and matrix density of compressed articular cartilage. *Arch. Biochem. Biophys.* 442:1–10.

27. Roberts, S., J. P. Urban, H. Evans, and S. M. Eisenstein. 1996. Transport properties of the human cartilage endplate in relation to its composition and calcification. *Spine.* 21:415–420.

28. Farndale, R. W., D. J. Buttle, and A. J. Barrett. 1986. Improved quantitation and discrimination of sulphated glycosaminoglycans by use of dimethylmethylene blue. *Biochim. Biophys. Acta.* 883:173–177.

29. Krishnan, R., E. N. Mariner, and G. A. Ateshian. 2005. Effect of dynamic loading on the frictional response of bovine articular cartilage. *J. Biomech.* 38:1665–1673.

30. Mow, V. C., M. H. Holmes, and W. M. Lai. 1984. Fluid transport and mechanical properties of articular cartilage: a review. *J. Biomech.* 17:377–394.

31. Brenner, H., and D. A. Edwards. 1993. Macrotransport Processes. Butterworth-Heinemann, Stoneham, MA.

32. Morel, V., and T. M. Quinn. 2004. Cartilage injury by ramp compression near the gel diffusion rate. *J. Orthop. Res.* 22:145–151.

33. Torzilli, P. A., T. C. Adams, and R. J. Mis. 1987. Transient solute diffusion in articular cartilage. *J. Biomech.* 20:203–214.

34. Torzilli, P. A., J. M. Arduino, J. D. Gregory, and M. Bansal. 1997. Effect of proteoglycan removal on solute mobility in articular cartilage. *J. Biomech.* 30:895–902.

35. Garcia, A. M., E. H. Frank, P. E. Grimshaw, and A. J. Grodzinsky. 1996. Contributions of fluid convection and electrical migration to transport in cartilage: relevance to loading. *Arch. Biochem. Biophys.* 333:317–325.

36. Allhands, R. V., P. A. Torzilli, and F. A. Kallfelz. 1984. Measurement of diffusion of uncharged molecules in articular cartilage. *Cornell Vet.* 74:111–123.

37. Maroudas, A. 1970. Distribution and diffusion of solutes in articular cartilage. *Biophys. J.* 10:365–379.

38. Mobasheri, A., S. J. Vannucci, C. A. Bondy, S. D. Carter, J. F. Innes, M. F. Arteaga, E. Trujillo, I. Ferraz, M. Shakibaei, and P. Martin-Vasallo. 2002. Glucose transport and metabolism in chondrocytes: a key to understanding chondrogenesis, skeletal development and cartilage degradation in osteoarthritis. *Histol. Histopathol.* 17:1239–1267.

39. Urban, J. P. G., S. Holm, A. Maroudas, and A. Nachemson. 1982. Nutrition of the intervertebral disk: effect of fluid flow on solute transport. *Clin. Orthop.* 170:296–302.

40. Sengers, B. G., H. K. Heywood, D. A. Lee, C. W. Oomens, and D. L. Bader. 2005. Nutrient utilization by bovine articular chondrocytes: a combined experimental and theoretical approach. *J. Biomech. Eng.* 127:758–766.